Louise Grant, Kirsty D. Shearer, Alicja Czopek, Emma K. Lees, Carl Owen, Abdelali Agouni, James Workman, Cristina Martin-Granados, John V. Forrester, Heather M. Wilson, Nimesh Mody, and Mirela Delibegovic

Myeloid-Cell Protein Tyrosine Phosphatase-1B Deficiency in Mice Protects Against High-Fat Diet and Lipopolysaccharide-Induced Inflammation, Hyperinsulinemia, and Endotoxemia Through an IL-10 STAT3-Dependent Mechanism

Protein tyrosine phosphatase-1B (PTP1B) negatively regulates insulin and leptin signaling, rendering it an attractive drug target for treatment of obesity-induced insulin resistance. However, some studies suggest caution when targeting macrophage PTP1B, due to its potential anti-inflammatory role. We assessed the role of macrophage PTP1B in inflammation and whole-body metabolism using myeloid-cell (LysM) PTP1B knockout mice (LysM PTP1B). LysM PTP1B mice were protected against lipopolysaccharide (LPS)-induced endotoxemia and hepatic damage associated with decreased proinflammatory cytokine secretion in vivo. In vitro, LPS-treated LysM PTP1B bone marrow–derived macrophages (BMDMs) displayed increased interleukin (*IL*)-*10* mRNA expression, with a concomitant decrease in *TNF-α* mRNA levels. These anti-inflammatory effects were associated with increased LPS- and IL-10–induced STAT3 phosphorylation in LysM PTP1B BMDMs. Chronic inflammation induced by high-fat (HF) feeding led to equally beneficial effects of macrophage PTP1B deficiency; LysM PTP1B mice exhibited improved glucose and insulin tolerance, protection against LPS-induced hyperinsulinemia, decreased macrophage infiltration into adipose tissue, and decreased liver damage. HF-fed LysM PTP1B mice had increased basal and LPS-induced IL-10 levels, associated with elevated STAT3 phosphorylation in splenic cells, *IL-10* mRNA expression, and expansion of cells expressing myeloid markers. These increased IL-10 levels negatively correlated with circulating insulin and alanine transferase levels. Our studies implicate myeloid PTP1B in negative regulation of STAT3/IL-10–mediated signaling, highlighting its inhibition as a potential anti-inflammatory and antidiabetic target in obesity.

Diabetes 2014;63:456–470 | DOI: 10.2337/db13-0885

Protein tyrosine phosphatase-1B (PTP1B) is a non-receptor tyrosine phosphatase, identified as an attractive drug target for conditions associated with metabolic

Institute of Medical Sciences, University of Aberdeen, College of Life Sciences and Medicine, Foresterhill Health Campus, Aberdeen, United Kingdom

Corresponding authors: Mirela Delibegovic, m.delibegovic@abdn.ac.uk, and Nimesh Mody, n.mody@abdn.ac.uk.

Received 5 June 2013 and accepted 28 October 2013.

This article contains Supplementary Data online at http://diabetes.diabetesjournals.org/lookup/suppl/doi:10.2337/db13-0885/-/DC1.

syndrome as well as potential anticancer therapeutic due to its diverse involvement in regulation of various cell signaling cascades. Evidence to support the notion that PTP1B inhibition may be beneficial in states of overnutrition and insulin resistance was demonstrated in mice with a global- (1,2) as well as tissue-specific PTP1B deletion (3–6).

Insulin resistance in adipose, muscle, and liver is exacerbated in obese states, due to the underlying presence of chronic low-grade inflammation and macrophage infiltration into these tissues. White adipose tissue (WAT) from obese subjects contains greater numbers of infiltrating proinflammatory macrophages in comparison with lean counterparts, and these cells secrete cytokines such as tumor necrosis factor-α (TNF-α), interleukin (IL)-1β, and IL-6, which can impair systemic insulin sensitivity (7–11). This process is enhanced further by the release of chemokines, such as monocyte chemoattractant protein-1, which recruits more activated tissue-macrophages into WAT (12). Saturated fatty acids are able to directly induce the expression of these proinflammatory cytokines via activation of the nuclear factor (NF)-κB pathway, and the receptor primarily responsible for potentiating this effect has been identified as the macrophage toll-like receptor (TLR)-4 (13). Mice with myeloid-TLR-4 deletion are protected against high-fat diet (HFD)-induced inflammation, adipose macrophage infiltration, and insulin resistance (14).

It has been postulated that PTP1B may act as a negative regulator of TLR-4 signaling in macrophages since in vitro PTP1B knockdown in the RAW 264.7 macrophage cell line resulted in elevated production of TNF-α, IL-6, and interferon (IFN)-β following challenge with a variety of TLR ligands (15). PTP1B overexpression in the same cell line caused a concomitant decrease in proinflammatory cytokine production in response to lipopolysaccharide (LPS) and palmitate challenge (15,16). Similarly, splenic macrophages isolated from global PTP1B$^{-/-}$ mice were found to be highly sensitive to LPS-induced inducible nitric oxide synthase (iNOS) expression and nitric oxide production, in addition to elevated IFN-γ–induced phosphorylation of STAT1 (17). In the same study, in vivo LPS-challenge increased sensitivity to endotoxic-shock in PTP1B$^{-/-}$ mice, associated with increased systemic production of IL-12 and IFN-γ. However, since these studies were performed in mice with global PTP1B deletion, and PTP1B regulation of cell function/signaling varies in a cell-specific manner (3–6), we set out to definitively establish the in vivo role of macrophage PTP1B by assessing the regulation of inflammation and whole-body metabolism in LysM PTP1B knockout mice.

RESEARCH DESIGN AND METHODS

Animal Studies

All animal procedures were performed under a project license approved by the U.K. Home Office under the Animals (Scientific Procedures) Act 1986 (PPL60/3951). PTP1B$^{fl/fl}$ and mice expressing Cre recombinase (Cre) under the control of the LysM promoter have been described previously (3). To generate myeloid PTP1B$^{-/-}$ mice, PTP1B$^{fl/fl}$ mice were crossed with LysM Cre mice (18) and back crossed nine times to pure C57BL/6J mice. DNA extraction and genotyping were performed as described previously (3). Age-matched male mice were studied and compared with PTP1B$^{fl/fl}$ and LysM Cre control littermates. Mice were group housed and maintained at 22–24°C on 12-h light/dark cycle with free access to food/water. At weaning (21 days), mice were placed on standard 3.4% fat chow-pellet diet (Rat and Mouse Breeder and Grower, Special Diets Services, DBM Food Hygiene Supplies, Broxburn, U.K.) or HFD (Adjusted Calories Diet, 55% fat, Harlan Teklad) for 29 weeks and weight recorded weekly. The approximate fatty-acid profile of Adjusted Calories Diet (percentage total fat) was 28% saturated, 30% *trans*, 28% monounsaturated (*cis*), and 14% polyunsaturated (*cis*). For endotoxemia experiments, 50-week-old chow-fed and high-fat (HF)-fed mice were fasted for 2 h and injected intraperitoneally with LPS (1 and 0.5 mg/kg, respectively; Merck). Mice were observed for signs of sepsis, including reduced mobility, fur ruffling, and conjunctivitis (19). At 24 or 3 h post-LPS injection (stated in figure legends), mice were killed by cervical dislocation and tissues/blood were harvested (3).

Blood Analysis

Tail-blood glucose from fasted (5 h) mice was measured using glucometers (Accu-Chek, Burgess Hill, U.K.) (6). Serum TNF-α, IL-6, monocyte chemoattractant protein-1, insulin, leptin, plasminogen activator inhibitor-1, and resistin were measured using adipokine multiplex kit (Millipore, U.K.), and serum IL-10 levels were determined by ELISA (R&D Systems, Minneapolis, MN). Alanine aminotransferase (ALT; BioVision) and serum glucose (Thermo Scientific) levels were assayed per the manufacturer's instructions. Glucose tolerance tests (GTTs) and insulin tolerance tests (ITTs) were performed as previously described (2,6). For hematocrit-level determination, whole blood was collected in heparinized microhematocrit capillary tubes and centrifuged for 3 min. The percentage hematocrit value was determined by measuring the length of the red blood cell layer and calculating as a percentage of the total height of the column sample.

Isolation of T-cells

Single-cell suspensions were made from spleens and lymph nodes by pressing through a 70 μm strainer (BD Falcon). After red blood cell lysis (Sigma), cells were labeled with anti-L3T4 (CD4) microbeads (Milteny Biotec) and sorted using LS-Columns (Milteny Biotec).

Isolation and Stimulation of Bone Marrow–Derived Macrophages

Bone marrow–derived macrophages (BMDMs) were obtained by flushing out femurs and tibiae with sterile

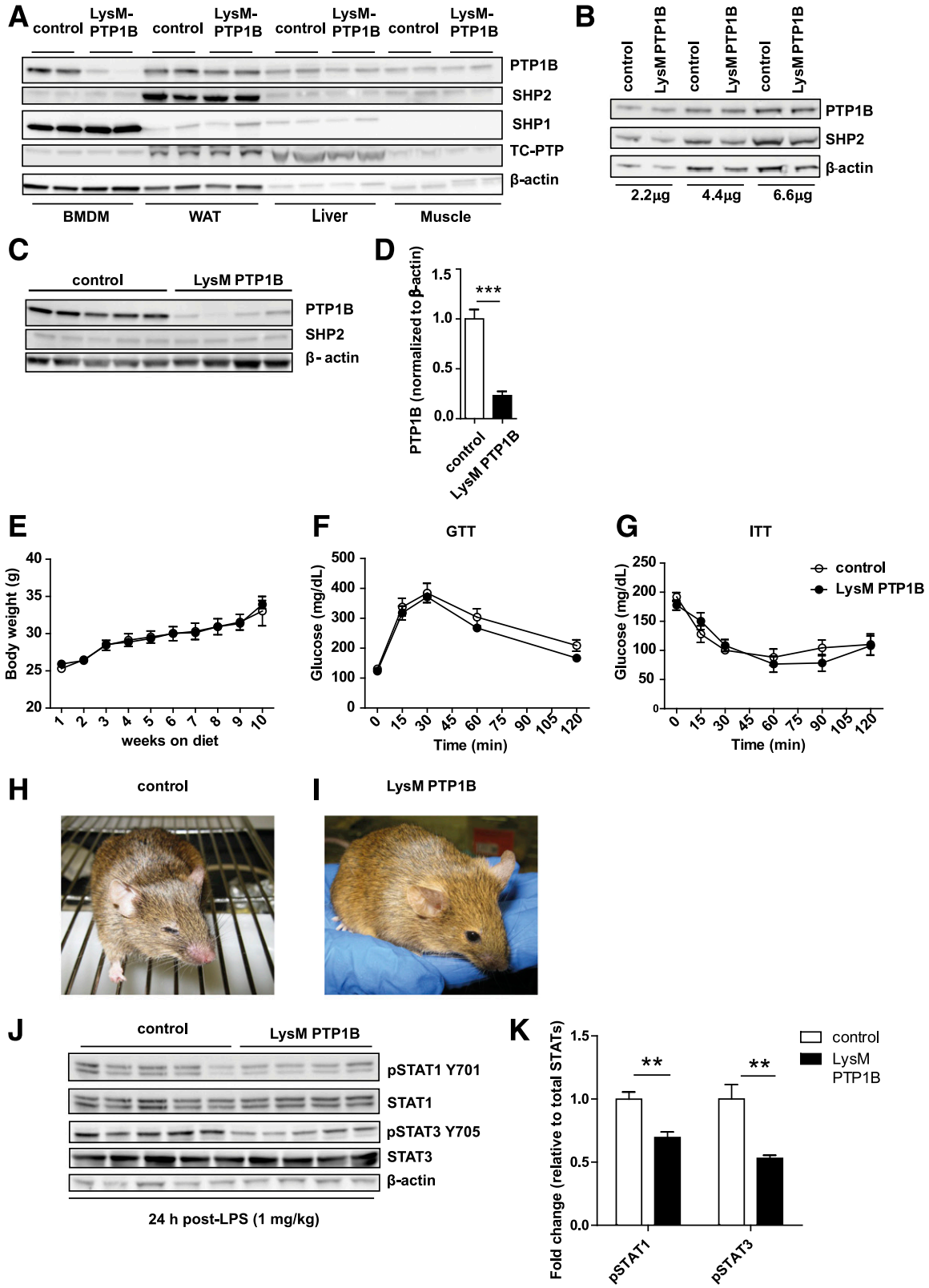

Figure 1—LysM PTP1B mice have unaltered glucose homeostasis but display an anti-inflammatory phenotype following in vivo challenge with low-dose LPS when compared with control littermates. *A*: Immunoblot depicting macrophage-specific deletion of PTP1B in LysM PTP1B mice fed chow diet compared with littermate controls. Tissues shown are (*left to right*) BMDM, WAT, liver, and muscle. Blot was reprobed for SHP2, SHP1, and T-cell protein tyrosine phosphatase in addition to β-actin as a loading control to confirm specificity of PTP1B deletion. *B*: PTP1B levels were maintained in CD4+ T-cells harvested from LysM PTP1B mice and were not different from control cells. *C*: Immunoblot displaying PTP1B, SHP2, and β-actin protein levels in BMDM isolated from control mice ($n = 5$) compared with LysM PTP1B ($n = 4$). *D*: Corresponding quantification data of PTP1B protein levels relative to β-actin, demonstrating a PTP1B deletion efficiency

Table 1—Fed and fasted metabolic parameters (chow)

Analyte	Genotype	Fed levels	Significance level	Fasted levels	Significance level
Chow diet					
Glucose (mg/dL)	Control	165.21 ± 10.79	$P = 0.14$	112.87 ± 10.16	$P = 0.69$
	LysM PTP1B	143.49 ± 4.87		106.89 ± 9.87	
Insulin (ng/mL)	Control	3.09 ± 0.20	$P = 0.93$	0.67 ± 0.12	$P = 0.59$
	LysM PTP1B	3.16 ± 0.90		0.76 ± 0.11	
Leptin (ng/mL)	Control	13.25 ± 1.41	$P = 0.09$	5.44 ± 0.99	$P = 0.11$
	LysM PTP1B	17.33 ± 1.43		8.40 ± 1.29	
Free fatty acids (mmol/L)	Control	1.51 ± 0.11	$P = 0.28$	2.55 ± 0.13	$P = 0.37$
	LysM PTP1B	1.35 ± 0.07		2.78 ± 0.23	
HFD					
Glucose (mg/dL)	Control	172.6 ± 5.39	$P = 0.86$	177.0 ± 12.37	$P = 0.33$
	LysM PTP1B	174.5 ± 9.83		197.0 ± 5.60	
Insulin (ng/mL)	Control	3.92 ± 0.38	$P = 0.25$	1.32 ± 0.22	$P = 0.71$
	LysM PTP1B	3.14 ± 0.44		1.17 ± 0.25	
Leptin (ng/mL)	Control	23.84 ± 1.85	$P = 0.69$	14.38 ± 1.67	$P = 0.56$
	LysM PTP1B	25.28 ± 3.37		16.60 ± 4.27	
Free fatty acids (mmol/L)	Control	1.54 ± 0.05	$P = 0.86$	1.65 ± 0.04	$P = 0.46$
	LysM PTP1B	1.52 ± 0.13		2.02 ± 0.80	

Data from chow-fed control ($n = 5$) or LysM PTP1B ($n = 4$) mice and HFD-fed control ($n = 12$) and LysM PTP1B ($n = 6$) mice are represented as mean ± SEM. Data were analyzed using two-tailed Student's t test ($P < 0.05$).

PBS (Lonza), as described previously (6). Mature macrophages were seeded in six-well tissue-culture plates (1×10^6 cells/well) and serum starved for 16 h prior to stimulation with 100 ng/ml LPS (InvivoGen), 10 ng/ml IL-10 (Peprotech), or 20 ng/ml IL-6 (Peprotech).

PTP1B Stable Knockdown Macrophages

Stable knockdown of PTP1B in RAW 264.7 cells (murine-macrophage cell line) was performed using short-hairpin RNA constructs as previously described (20).

Immunoblotting

Cells and tissues were lysed in radioimmunoprecipitation assay buffer containing fresh sodium orthovanadate and protease inhibitors (21). Proteins were separated by 4–12% SDS-PAGE and transferred to nitrocellulose membranes. Immunoblots were performed using antibodies from cell signaling (New England Biolabs, Hitchin, U.K.; unless stated otherwise) against phosphorylated extracellular signal–related kinase (ERK)1/2, mitogen-activated protein kinase (MAPK) T202/Y204, phosphorylated IκB kinase (IKK) α/β S176/S180, IκBα, p-c-jun S63, phosphorylated P38 T180/Y182, phosphorylated STAT1 Y701, phosphorylated STAT3 Y705, STAT3, BCL-2, iNOS, SHP1, phosphorylated Akt/PKBS473, phosphorylated S6 ribosomal protein S235/236, phosphorylated GSK 3α/β, phosphorylated IR Y1162/1163 (Invitrogen), SHP2 (Santa Cruz), ERK2 (Santa Cruz), T-cell protein tyrosine phosphatase (R&D Systems), phosphorylated JNK/SAPK T183/Y185 (R&D Systems), β-actin (Sigma), and PTP1B (Millipore). Immunoblots were visualized using enhanced chemiluminescence and quantified by densitometry scanning using Bio1D-software (PeqLab, Fareham, U.K.).

Gene Expression Analysis

Cells/tissues were homogenized in TriFast reagent (Peqlab, Sarisbury Green, U.K.) (20). cDNA synthesis was carried out from 1 μg of RNA using Tetro cDNA-synthesis kit (Bioline). Quantitative real-time PCR was performed using Light-Cycler 480 (Roche), and gene expression of *iNOS*, *TNF-α*, *IL-6*, *MCP1*, *IL-1β*, *IL-1α*, *IL-10*, and *BCL2* was determined relative to the most stable

of 77% in LysM PTP1B BMDM compared with control levels. *E*: Mean body weight of male mice that had been back crossed to C57BL/6J background for nine generations was unchanged when LysM PTP1B ($n = 6$) were compared with control littermates fed standard 3.4% fat chow pellet diet for 10 weeks after weaning ($n = 6$). *F* and *G*: GTTs revealed no differences in the ability of LysM PTP1B to clear glucose when compared with control mice (*F*), and ITTs demonstrated no differences between genotypes (*G*). Forty-eight-week-old control mice ($n = 5$) and LysM PTP1B littermates ($n = 4$) were injected with 1 mg/kg LPS intraperitoneally. Photographs showing an example of a control mouse (*H*) compared with a LysM PTP1B mouse (*I*) 24 h after receiving 1 mg/kg LPS. Control mice exhibited more severe signs of endotoxic shock compared with mutant mice, which were in better health. *J*: Phosphorylation levels of STAT1 (Y701) and STAT3 (Y705) in liver tissue harvested following LPS injection were lower in LysM PTP1B mice compared with controls. *K*: Control, white bars; LysM PTP1B, black bars. Data are expressed as mean ± SEM. TC-PTP, T-cell protein tyrosine phosphatase; pSTAT, phosphorylated STAT. $^{**}P < 0.01$, $^{***}P < 0.001$.

Table 2—Analysis of serum obtained from control and LysM PTP1B 3 and 24 h following 1 mg/kg LPS injection

Analyte (ng/mL)	Genotype	3 h post-LPS	Significance level	24 h post-LPS	Significance level
CHOW					
TNF-α	Control	0.38 ± 0.03	$P = 0.38$	0.10 ± 0.03	$P = 0.18$
	LysM PTP1B	0.47 ± 0.07		0.04 ± 0.005	
IL-6	Control	149.0 ± 10.31	$P = 0.25$	14.3 ± 5.3	$P = 0.09$
	LysM PTP1B	134.4 ± 12.30		3.7 ± 0.9	
IL-10	Control	0.67 ± 0.03	$P = 0.12$	0.73 ± 0.13	$P = 0.7$
	LysM PTP1B	0.89 ± 0.12		0.65 ± 0.07	
MCP-1	Control	ND		3.46 ± 1.60	$P = 0.3$
	LysM PTP1B	ND		1.54 ± 1.80	
Insulin	Control	ND		3.30 ± 0.96	$P = 0.5$
	LysM PTP1B	ND		2.50 ± 0.36	
Resistin	Control	ND		7.54 ± 1.87	$P = 0.5$
	LysM PTP1B	ND		6.00 ± 0.84	
PAI-1	Control	ND		7.41 ± 0.65	$P = 0.08$
	LysM PTP1B	ND		11.71 ± 1.90	
Analyte (ng/mL)	**Genotype**	**Basal**	**Significance level**	**3 h post-LPS**	**Significance level**
HFD					
TNF-α	Control	ND		1.44 ± 0.28	$P = 0.2$
	LysM PTP1B	ND		2.10 ± 0.30	
IL-6	Control	0.03 ± 0.004	$P = 0.07$	60.78 ± 4.45	$P = 0.5$
	LysM PTP1B	0.11 ± 0.07		54.98 ± 10.41	
MCP-1	Control	0.06 ± 0.006	$P = 0.1$	55.99 ± 25.43	$P = 0.5$
	LysM PTP1B	0.04 ± 0.01		31.46 ± 14.46	
PAI-1	Control	5.00 ± 1.14	$P = 0.3$	5.15 ± 0.43	$P = 0.09$
	LysM PTP1B	6.88 ± 1.06		7.84 ± 1.97	

Data from 3 h ($n = 6$ per genotype) and 24 h (control mice, $n = 5$; LysM PTP1B, $n = 4$) LPS-injected mice. Multiplex analysis was used for 24 h time points (TNF-α, IL-6, insulin, resistin, plasminogen activator inhibitor 1 [PAI-1]) and ELISA used for the remaining time points/analytes. Data are represented as mean ± SEM and analyzed using two-tailed Student's *t* test ($P < 0.05$). ND, not determined or too low to detect.

reference gene (*YWhaz*, *NoNo*, or *β-actin*), which was identified using a Web-based reference gene assessment tool (http://www.leonxie.com/referencegene.php?type=reference). Primer sequences are provided in the Supplementary Data online.

Cytokine Quantification

TNF-α, *IL-6*, and *IL-10* concentrations in BMDM supernatants were quantified by ELISA (R&D Systems) or multiplex ELISA (Millipore), according to the manufacturers' instructions.

Nitrite Determination

Nitric oxide production by BMDMs was quantified by determining the concentration of nitrite present in supernatants using Griess reaction (22).

Adipose Immunohistochemical Staining

Ethanol-fixed, paraffin-embedded adipose tissue sections were stained as previously described (23) using rat antimouse F4/80 (AbD Serotec MCA497RT), CD68 (Abcam ab31630), and iNOS (Cell Signaling).

Hematoxylin and Eosin Staining

Liver and spleen tissue was fixed in formaldehyde, embedded in paraffin, sectioned, and stained with hematoxylin and eosin.

Flow Cytometry

Single-cell suspensions were made by pressing spleens through cell strainers, and cell suspensions were centrifuged at 900*g* for 5 min. Red blood cells were lysed for 1 min with red blood cell lysis buffer (Sigma) and washed by centrifugation at 900*g* for 5 min in PBS without Ca^{2+} and Mg^{2+}, 5% fetal bovine serum, and 5 mmol/L EDTA. We blocked 1×10^6 cells per label for 30 min in the dark with rat anti-mouse CD16/CD32 (BD, 0.5 μg/reaction) and then labeled them with optimized quantities of antibodies (PerCP-Cy5.5 [BD 550954], CD8 V450 [BD 560469], CD3 AF488 [BD 557666], CD45 PE [BD 553089], CD11b AF488 [BD 557672], CD11c V450 [BD 560521], Gr1 APC-Cy7 [BD 557661], MHC-II PE [BD 557000], Ly6C PerCP-Cy5.5 [BD 560602], Ly6G APC [BD 560595], F4/80-AF647 [AbD Serotech]). Data were acquired on BD LSR II and analyzed using DiVa software.

Data Analysis

Data are expressed as mean ± SEM. Statistical analyses were performed using correlation analyses, one-way ANOVA with Tukey's multiple comparison post-tests, two-way ANOVA with Bonferroni multiple comparisons post-tests, and two-tailed Student's *t* tests, as appropriate, using GraphPad Prism 5 statistical software.

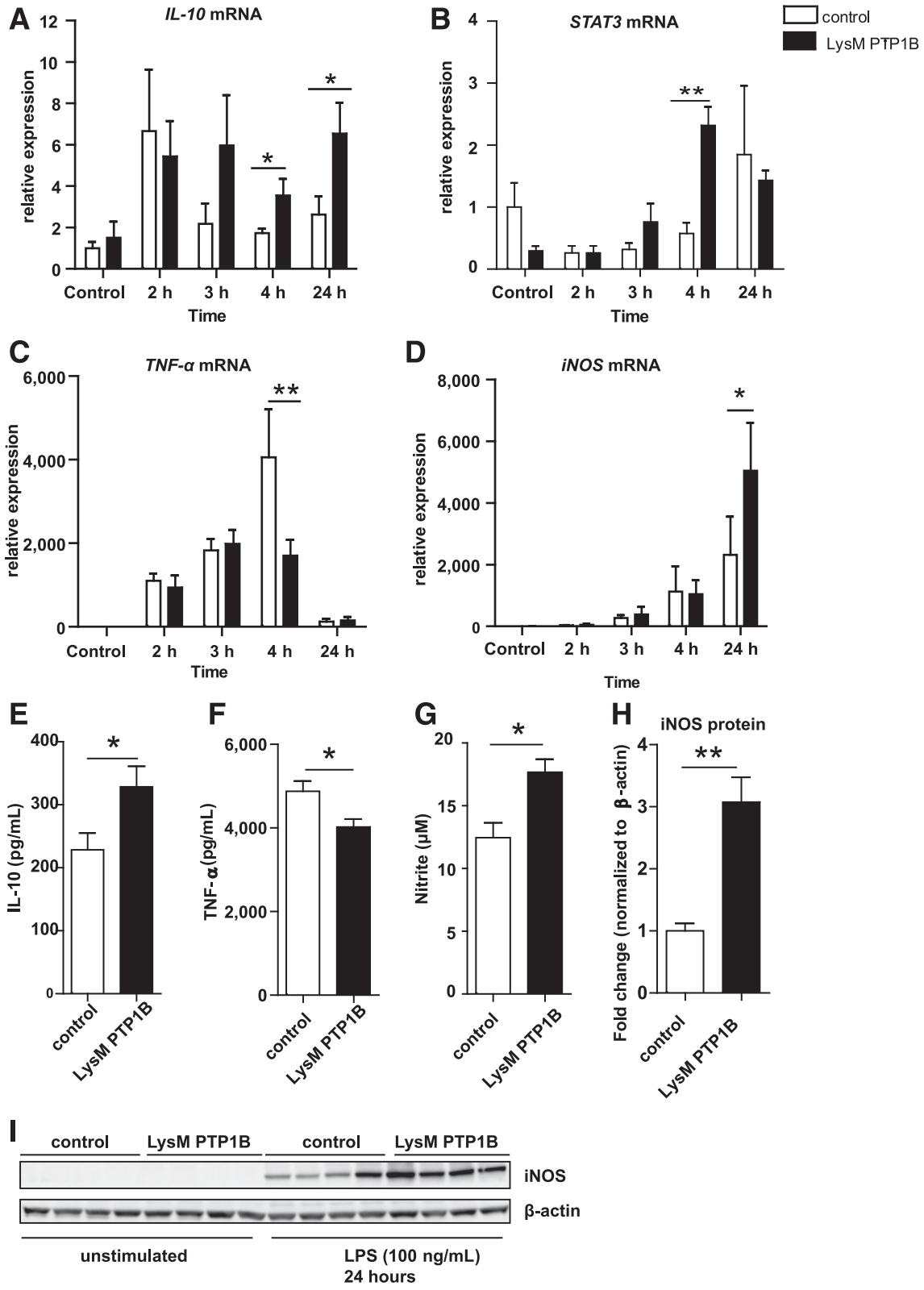

Figure 2—BMDMs isolated from LysM PTP1B have increased IL-10 and iNOS and decreased TNF-α gene expression and protein in response to LPS. Treatment of BMDMs isolated from LysM PTP1B mice (n = 4) and control mice (n = 4) with 100 ng/ml LPS for 4 and 24 h revealed an increase in *IL-10* mRNA levels ($P \leq 0.05$; one-tailed t test) (*A*) and *STAT3* mRNA levels (4 h post-LPS, $P \leq 0.01$; two-tailed t test) (*B*) in the absence of PTP1B. *C*: Levels of proinflammatory *TNF-α* transcripts were downregulated in LysM PTP1B cells compared with control cells following 4 h challenge with LPS ($P \leq 0.05$; two-tailed t test). *D*: *iNOS* mRNA expression was elevated in LysM PTP1B BMDMs following 4 h LPS challenge ($P \leq 0.05$, respectively; two-tailed t test). Expression levels were calculated relative to the most stable reference genes (*β-actin*, *YWhaz*, or *NoNo*). *E* and *F*: Supernatants harvested from LysM PTP1B macrophages following 6 h treatment with 100 ng/ml LPS contained higher levels of IL-10 (*E*) and lower levels of TNF-α (*F*) compared with control supernatants ($P \leq 0.05$; two-tailed

RESULTS

LysM PTP1B Mice Are Protected Against LPS-Induced Endotoxemia

PTP1B deletion was achieved in BMDMs isolated from LysM PTP1B mice, without affecting PTP1B levels in WAT, liver, muscle (Fig. 1*A*) or $CD4^+$ T-cells (Fig. 1*B*). A deletion efficiency of ~75% was determined in LysM PTP1B BMDMs (n = 4) compared with controls (n = 5) (Fig. 1*C* and *D*). There were no body weight differences (Fig. 1*E*), and glucose (GTT) and insulin (ITT) tolerance were unaltered between LysM PTP1B and control mice on chow diet (Fig. 1*F* and *G*, respectively). Fed and fasted metabolic parameters were unchanged in the absence of myeloid PTP1B (Table 1). To establish whether macrophage PTP1B plays a role in TLR-4 signaling, LysM PTP1B mice with confirmed PTP1B deletion (Fig. 1*C*) and littermate controls were injected with low-dose LPS (1 mg/kg), and their response to endotoxin was monitored. Twenty-four hours post-LPS, control mice exhibited obvious signs of endotoxemia, including closed eyes, shivering, reduced mobility, and ruffled fur (Fig. 1*H* and Supplementary Videos 1 and 2), whereas LysM PTP1B littermates were completely protected (Fig. 1*I* and Supplementary Videos 3 and 4). LysM PTP1B mice had decreased serum TNF-α and IL-6 levels compared with controls, although this did not reach significance (TNF-α, 0.04 ± 0.005 vs. 0.1 ± 0.03 ng/ml, respectively [P = 0.18; two-tailed t test]; IL-6, 3.7 ± 0.9 vs. 14.3 ± 5.3 ng/ml, respectively [P = 0.06; two-tailed t test]) (Table 2). At 3 h post-LPS, there was also a trend toward increased IL-10 levels in LysM PTP1B mice (0.89 ± 0.12 vs. 0.67 ± 0.03 ng/ml [P = 0.12; two-tailed t test]), although this was not observed at 24 h post-LPS (Table 2). Furthermore, levels of hepatic STAT1 and STAT3 phosphorylation were significantly lower in LysM PTP1B mice, indicative of decreased LPS-induced hepatic inflammation (Fig. 1*J* and *K*).

LysM PTP1B Macrophages Exhibit Altered Cytokine Kinetics

To assess whether the anti-inflammatory phenotype observed in LPS-challenged LysM PTP1B mice is due specifically to the absence of macrophage PTP1B, isolated BMDMs were stimulated with 100 ng/ml LPS for varying durations up to 24 h in vitro.

Elevations in *IL-10* mRNA expression in LysM PTP1B BMDMs following LPS stimulation were observed at both 4 and 24 h (Fig. 2*A*), which was associated with increased STAT3 mRNA expression 4 h post-LPS treatment (Fig. 2*B*). *TNF-α* transcript levels were concomitantly downregulated following 4 h of LPS treatment in LysM PTP1B cells (Fig. 2*C*). Supplementary Table 1 displays additional measures of proinflammatory cytokines and markers of M1 and M2 macrophages.

In keeping with previously published data showing that isolated macrophages from global $PTP1B^{-/-}$ mice are highly sensitive to LPS-induced *iNOS* expression (17), we also found increased levels of LPS-stimulated *iNOS* mRNA transcript in the absence of macrophage PTP1B (Fig. 2*D*). Supernatants harvested from LysM PTP1B BMDMs challenged with LPS for 6 h contained increased IL-10 (Fig. 2*E*) and decreased TNF-α levels (Fig. 2*F*). Supernatant nitrite (Fig. 2*G*) and iNOS protein levels (Fig. 2*H* and *I*) were higher in LPS-stimulated LysM PTP1B macrophages compared with respective control cells.

Macrophage PTP1B Regulates Janus Kinase/STAT Signaling in LPS- and IL-10–Treated LysM PTP1B Macrophages and RAW 264.7 Stable Knockdown Cells

We found increased levels of phosphorylated STAT1 α and β isoforms in LysM PTP1B macrophages treated with LPS for 24 h (Fig. 3*A* and *C*), which is in agreement with previous reports and is a likely explanation for the elevated iNOS and nitrite levels produced by these cells (17). The level of phosphorylated STAT3 was also significantly increased in LysM PTP1B cells following 24 h of treatment with 100 ng/ml LPS (Fig. 3*B* and *C*). The ability of endogenous IL-10 to directly induce STAT3 activation is a likely cause for the heightened levels of phosphorylated STAT3 observed in PTP1B-deficient macrophages since the levels of IL-10 detected in respective supernatants were also elevated (24).

To assess this, LysM PTP1B and control macrophages were stimulated with IL-10 for varying durations, and levels of STAT3 phosphorylation were determined (Fig. 3*D*). IL-6, which also activates STAT3, was used to allow for a direct comparison (Fig. 3*E*). An elevation in IL-10–induced phosphorylated STAT3 was observed following 60- and 120-min stimulation (Fig. 3*F*) in the absence of macrophage PTP1B, which was not the case for IL-6–induced STAT3 phosphorylation (data not shown). There was a negative correlation between PTP1B protein levels present in each cell batch (Fig. 3*G*) and the quantity of phosphorylated STAT3, following 120-min IL-10 treatment (Fig. 3*H*), suggesting a dose-dependent effect of STAT3 dephosphorylation by PTP1B. RAW 264.7 cells with PTP1B stable knockdown (Fig. 3*I*) also showed increased LPS-induced phosphorylated STAT1-Y701 (Fig. 3*J*), phosphorylated STAT3-Y705, and iNOS (Fig. 3*K*) and increased IL-10–induced phosphorylated STAT3-Y705 (Fig. 3*L*).

t test). *G*: Nitrite levels were increased in supernatants harvested from LysM PTP1B BMDMs stimulated for 24 h with 100 ng/ml LPS compared with respective controls ($P \leq 0.05$; two-tailed t test). *H* and *I*: Quantification (*H*) of immunoblot (*I*) showing elevated iNOS protein levels in LysM PTP1B compared with control BMDM cells following challenge with 100 ng/ml LPS for 24 h ($P \leq 0.05$; two-tailed t test). Control, white bars; LysM PTP1B, black bars. Data are expressed as mean ± SEM. $^*P < 0.05$, $^{**}P < 0.01$.

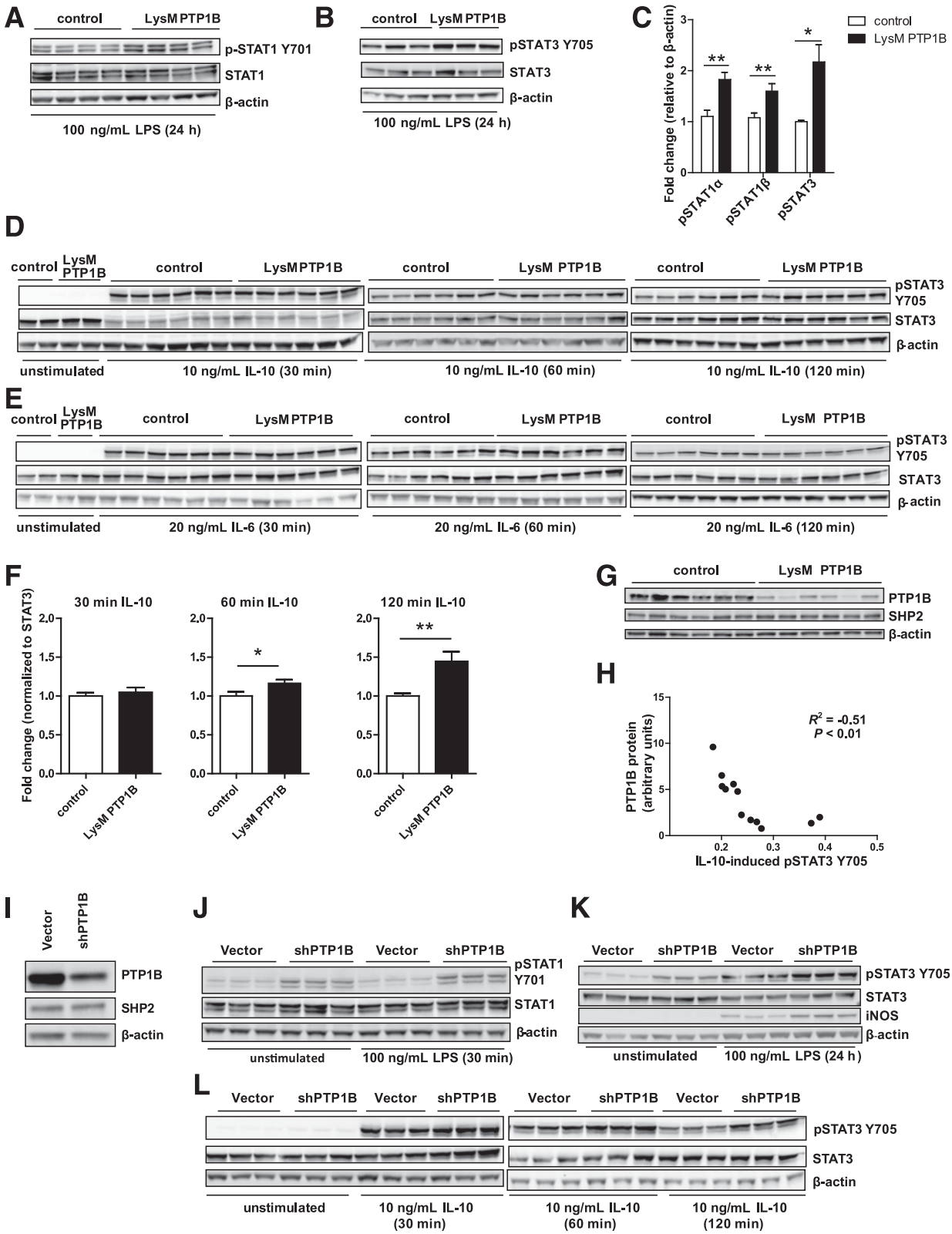

Figure 3—LysM PTP1B BMDMs and a RAW 264.7 macrophage cell line with PTP1B knockdown display increased LPS-induced phosphorylation of STAT1 and STAT3 and increased IL-10–induced phosphorylated STAT3 in vitro when compared with control cells. *A* and *B*: Immunoblot showing levels of phosphorylated STAT1 (Y701) (*A*) and phosphorylated STAT3 (Y705) (*B*) in control and LysM PTP1B BMDMs stimulated with 100 ng/ml LPS for 24 h. *C*: Levels of phosphorylated STAT1 α ($P \leq 0.01$; two-tailed *t* test) and β ($P \leq 0.01$; two-tailed *t* test) and phosphorylated STAT3 ($P \leq 0.05$; two-tailed *t* test) were elevated in LPS-treated LysM PTP1B BMDMs compared with control cells (phosphorylated STAT proteins are expressed relative to relevant total STAT protein). Immunoblot showing levels of phospho-STAT3 protein in LysM PTP1B and control BMDMs induced by 10 ng/ml IL-10 (*D*) and 20 ng/ml IL-6 (*E*) for 30, 60, and 120 min.

Previous studies implicated macrophage PTP1B in negative regulation of MAPK and NF-κB signaling cascades, initiated by various TLR ligands (15). In our study, macrophage PTP1B deficiency in vitro did not affect phosphorylation of c-Jun (component of MAPK signaling) (Supplementary Fig. 1) or phosphorylation of p65 (data not shown) and associated degradation of IκBα (components of NF-κB signaling) (Supplementary Fig. 1), following LPS stimulation at various time points. More detailed analysis of these pathways revealed no alterations in the levels of phosphorylated ERK1/2 (Supplementary Fig. 2), p38, JNK1/2, or IKK (Supplementary Fig. 3).

LysM PTP1B Mice Show Improved Glucose Homeostasis in a Model of HFD Feeding, Protection Against LPS-Induced Hyperinsulinemia, and Decreased WAT Inflammation and Hepatic Damage

Since LysM PTP1B mice were protected from an acute inflammatory challenge, we tested in vivo effects of myeloid PTP1B deficiency under states of chronic low-grade inflammation, caused by long-term (29 weeks) HFD feeding (23).

Despite no alterations in body weight (Fig. 4*A*), GTTs revealed improved ability to clear exogenous glucose in LysM PTP1B HFD-fed mice (Fig. 4*B*). The area under the curve (AUC) also confirmed that LysM PTP1B mice were more glucose tolerant than control mice (Fig. 4*C*). LysM PTP1B mice were also more insulin tolerant, with decreased blood glucose levels at 15, 90, and 120 min post-insulin injection (Fig. 4*D*) and decreased AUC during ITT (Fig. 4*E*).

Further, acute proinflammatory LPS challenge led to hyperinsulinemia in HFD-fed control mice (75% increase from basal). Strikingly, LysM PTP1B mice were completely protected against LPS-induced hyperinsulinemia (no increase from basal) (Fig. 4*F*) and post-LPS insulin levels were significantly lower in LysM PTP1B compared with control mice. Post-LPS blood glucose levels were also lower in LysM PTP1B mice (Fig. 4*G*). Additional measures of metabolic parameters and circulating cytokines are shown in Tables 1 and 2, respectively.

HFD-fed LysM PTP1B and control mice were injected with either saline or insulin (10 mU/g body weight), and components of the insulin signaling pathway were investigated in muscle, liver, and WAT. There were no significant differences in insulin-stimulated insulin receptor phosphorylation between the two genotypes in muscle (Fig. 4*H*), liver, or WAT (Supplementary Figs. 4 and 5, respectively).

F4/80 and CD68 immunohistochemical staining of WAT from HFD-fed LysM PTP1B mice revealed a trend toward decreased expression of these markers when compared with controls (Fig. 4*I*). To confirm this quantitatively, we performed quantitative RT-PCR analysis of WAT, which showed lower transcript levels of *F4/80* and *TNF-α* and a trend for decreased expression of *CD68* (P = 0.09; two-tailed t test) in LysM PTP1B mice (Fig. 4*J*), indicative of decreased macrophage infiltration into WAT and associated inflammation. HFD-fed LysM PTP1B mice also had lower levels of hepatic lipid accumulation (Fig. 4*K* and *L*), which was associated with decreased serum ALT levels in these mice (Fig. 4*M*), indicative of improved liver function. Furthermore, LysM PTP1B mice exhibited increased expression of the antiapoptotic gene *BCL2* (Fig. 4*N*).

HFD-Fed LysM PTP1B Mice Have Increased Circulating IL-10 Levels, an Elevation in Spleen Cells Expressing Myeloid Markers, and Increased Levels of Phosphorylated STAT3 in the Spleen

Basal circulating levels of the anti-inflammatory cytokine IL-10 were elevated in HFD-fed LysM PTP1B compared with control mice (Fig. 5*A*). Acute LPS challenge led to an induction of IL-10 in both control and LysM PTP1B mice, which led to a further 120% elevation in IL-10 levels in LysM PTP1B (Fig. 5*B*). Furthermore, we found a negative correlation between serum IL-10 and ALT levels (Fig. 5*C*), as well as serum IL-10 and insulin levels (Fig. 5*D*) in HFD mice following LPS injection, suggesting that elevated circulating IL-10 levels are strongly associated with the anti-inflammatory role of myeloid PTP1B deficiency.

Despite the strong anti-inflammatory phenotype of LysM PTP1B mice, these mice (but not control mice) developed splenomegaly on HFD (Fig. 5*E*), with a mean spleen weight of 0.48 ± 0.05 g (n = 14) compared with 0.14 ± 0.02 g (n = 13; $P \leq 0.0001$; two-tailed t test), which was also significant when corrected for body weight (Fig. 5*F*). To assess if these mice were anemic, hematocrit testing was performed on whole blood, and no differences were found between LysM PTP1B (36.6 ± 1.1%; n = 9) and control mice (38.9 ± 1.0%; n = 3). Hematoxylin and eosin staining of spleen sections

F: Increased IL-10 phosphorylated STAT3 relative to total STAT3 in LysM PTP1B BMDMs compared with control cells following 60-min ($P \leq 0.05$; two-tailed t test) and 120-min ($P \leq 0.01$; two-tailed t test) stimulation. *G* and *H*: Immunoblot displaying levels of PTP1B protein present in control and LysM PTP1B BMDMs used for IL-10 and IL-6 stimulations (*G*) and the correlation between PTP1B protein levels and levels of phosphorylated STAT3 following 120-min IL-10 stimulation ($R^2 = -0.51$; $P \leq 0.01$) (*H*). *I*: Immunoblot showing effective PTP1B knockdown in RAW 264.7 cells transfected with PTP1B short hairpin RNA compared with cells transfected with empty vector only. *J* and *K*: Increased levels of LPS-induced phosphorylated STAT1 (Tyr701) (*J*) and phosphorylated STAT3 (Tyr705) (*K*) and iNOS protein were observed for shPTP1B RAW 264.7 cells compared with vector-only cells. *L*: Levels of phosphorylated STAT3 (Tyr705) were also elevated in PTP1B short hairpin RNA RAW 264.7 cells treated with IL-10 during a time-course experiment (30, 60, and 120 min) when compared with levels in vector-only RAW 264.7 cells. Control, white bars; LysM PTP1B, black bars. Data are expressed as mean ± SEM. pSTAT, phosphorylated STAT; shPTP1B, PTP1B short hairpin RNA. *$P < 0.05$, **$P < 0.01$.

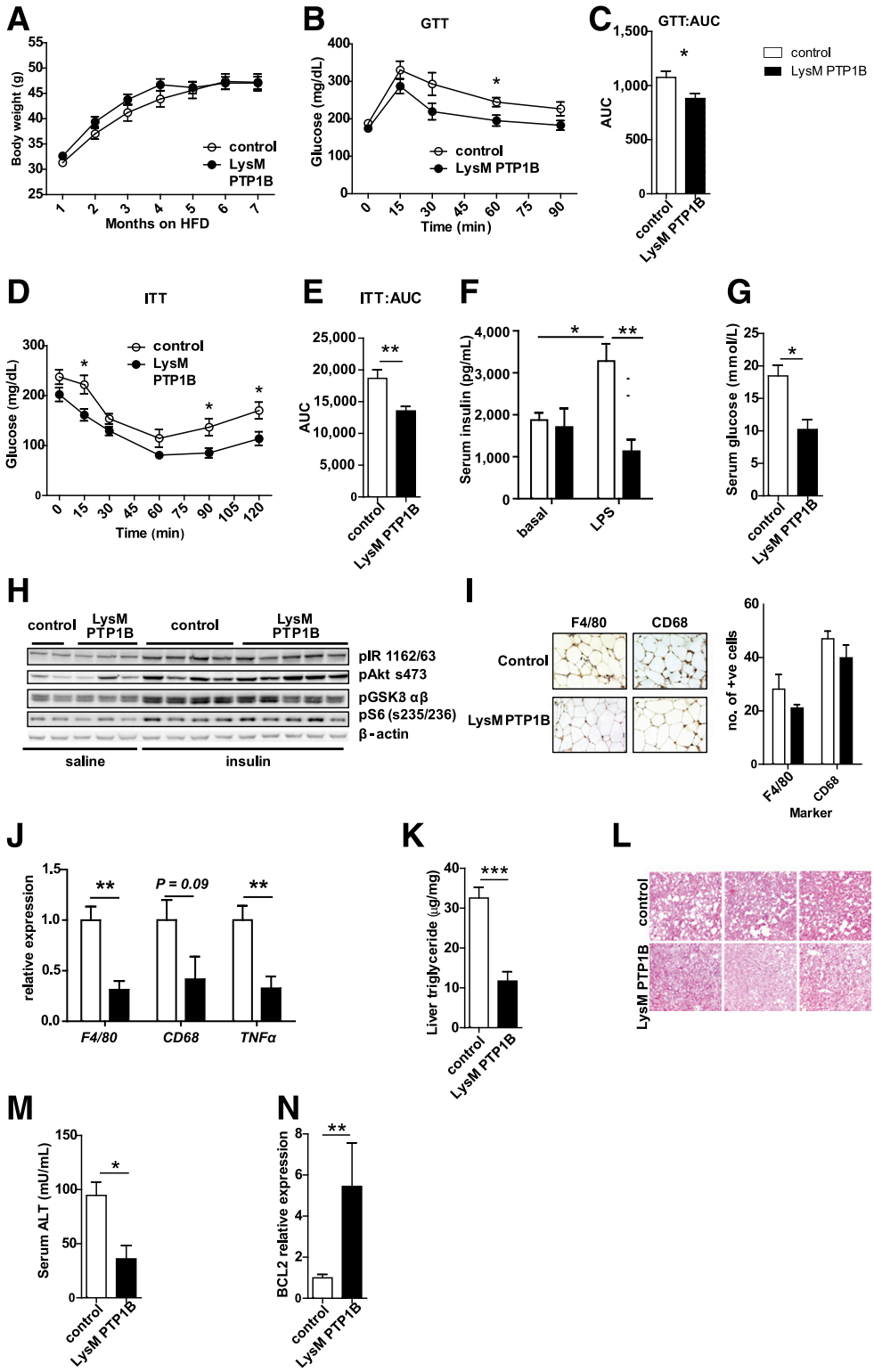

Figure 4—LysM PTP1B mice fed an HFD are more glucose and insulin tolerant than littermate controls despite no alteration in body weight, are protected against LPS-induced hyperinsulinemia, have decreased levels of adipose tissue inflammation, and have lower levels of HF-induced liver damage. *A*: Body weights for LysM PTP1B mice (n = 5) compared with control mice (n = 6) during an adjusted-calorie diet containing 55% fat (HFD). *B*: Following long-term HF dietary feeding, LysM PTP1B mice (n = 5) were more glucose tolerant than controls (n = 6) 60 min post-glucose injection as determined by GTT ($P \leq 0.05$; two-tailed t test). *C*: GTT results expressed as AUC showed significant improvement in glucose tolerance in the absence of PTP1B ($P \leq 0.05$; two-tailed t test). *D*: ITT of HF-fed LysM PTP1B mice (n = 8) revealed increased insulin tolerance compared with HF-fed control mice (n = 6) at 15, 90, and 120 min post-insulin (1.1 mU insulin/g body weight) infusion (two-way ANOVA). *E*: AUC for ITT was lower for LysM PTP1B mice compared with controls ($P \leq 0.01$; two-tailed t test). *F* and *G*: Three hours after administration of 0.5 mg/kg LPS, circulating insulin levels measured in HFD-fed control mice (n = 6) were significantly greater than basal levels ($P \leq 0.05$; two-tailed t test), but this was not observed for LysM PTP1B littermates (n = 5). LysM

revealed unremarkable histology (Fig. 5*G*). Spleen size was found to strongly correlate with circulating IL-10 levels under basal and LPS-stimulated states (Fig. 5*H* and *I*). Splenic IL-10 mRNA levels correlated with circulating IL-10 levels following LPS-treatment, suggesting that the elevation in systemic IL-10 seen in HFD-fed LysM PTP1B is, at least in part, spleen derived (Fig. 5*J*).

Flow cytometry analysis of splenocytes established that the percentage of cells expressing the granulocyte/monocyte marker Gr1 and the monocyte marker Ly6C were significantly increased in LysM PTP1B cells compared with controls, and a trend for increased expression of Ly6G was noted ($P = 0.09$) (Fig. 5*K*). There were no alterations in the percentage of cells expressing CD3, CD4, CD8, B220, CD11c, CD11b, F4/80, and MHCII; however, when normalized against total cell number, a significant increase in absolute cell numbers expressing all markers was established for LysM PTP1B mice compared with controls (Supplementary Table 1).

Spleen lysates from HFD-fed LysM PTP1B mice revealed an increase in the phosphorylation of STAT3α and STAT3β isoforms compared with control lysates (Fig. 5*L* and *M*). Using antibodies against total STAT3, a significant increase in the alternatively spliced STAT3β isoform was noted in LysM PTP1B mice (Fig. 5*L* and *M*). Interestingly, the splenic level of the antiapoptotic protein BCL2, which is regulated at the gene level by STAT3, was also increased in these mice, which could contribute toward the splenomegaly phenotype observed (Fig. 5*L* and *M*).

DISCUSSION

Previous reports have implicated macrophage PTP1B in the negative regulation of TLR-4-mediated inflammatory signaling; however, these studies have been restricted to in vitro cell line analysis or characterization of responses in PTP1B global knockout mice (15–17,25). To definitively address the role of macrophage PTP1B in inflammatory signaling, we have generated mice with myeloid-specific PTP1B deletion and interrogated their whole-body physiology and signaling in isolated macrophages. These mice exhibited an LPS-tolerant phenotype in vivo, which was mirrored by the attenuation of proinflammatory cytokine expression in LPS-treated BMDMs lacking PTP1B in vitro. A likely explanation for the downregulation of *TNF-α* observed in vitro was the concomitant increase in transcription and secretion of the anti-inflammatory cytokine, IL-10. This was further reinforced by heightened levels of phosphorylated STAT3, which is known to mediate IL-10–driven repression of inflammatory targets (26). A similar increase in phosphorylated STAT3 was observed when macrophages lacking PTP1B were challenged with IL-10 in vitro. The IL-10R engage Janus kinase (JAK)1 and Tyk2 following receptor activation, leading to the phosphorylation and activation of STAT3 (27,28), and since Tyk2 is a known substrate of PTP1B (29), this is a plausible reason for the hyperphosphorylation of STAT3 observed in the absence of PTP1B. Furthermore, activated STAT3 has been shown to control the expression of the IL-10 promoter, leading to a positive feedback mechanism (30). In summary, the altered cytokine profile displayed by these cells and their increased sensitivity to IL-10 may be responsible, at least in part, for the state of LPS tolerance observed in LysM PTP1B mice 24 h after receiving low-dose endotoxin in vivo.

Our in vitro analysis also revealed increased STAT1 phosphorylation, leading to increased iNOS and nitrite production in LPS-treated LysM PTP1B BMDMs, which is in agreement with previous findings of LPS-treated spleen-macrophages from global knockout mice (17). Although heightened levels of nitric oxide have been partly implicated as a cause for increased endotoxin sensitivity in PTP1B$^{-/-}$ mice, no such phenotype was observed in LysM PTP1B mice. These findings do, however, add to a large body of evidence that links PTP1B to the regulation of JAK STAT activation (3,29,31–34).

The anti-inflammatory phenotype observed in endotoxin-challenged LysM PTP1B mice was similarly replicated in our long-term HFD-feeding study, which is known to chronically increase plasma LPS concentration and has thus been termed metabolic endotoxemia (23). Most remarkably, in vivo LysM PTP1B mice exhibited increased basal and LPS-induced levels of circulating IL-10 compared with control animals, which we found to negatively correlate with insulin and ALT levels. The insulin-sensitizing effect mediated by IL-10 has been widely documented before. Low circulating levels of IL-10

PTP1B mice had significantly lower circulating insulin ($P \leq 0.01$; two-tailed *t* test) (*F*) and glucose (*G*) ($P \leq 0.05$; two-tailed *t* test) than control mice following LPS injection. *H*: Muscle tissue immunoblot of insulin signaling pathway components after saline or insulin (10 mU/g body weight) injection of control or LysM PTP1B mice. *I*: Representative images of control and LysM PTP1B adipose tissue stained with F4/80 and CD68 and corresponding quantification data. *J*: RT-PCR analysis of HF-fed mice revealed lower mRNA expression of *F4/80* and *TNF-α* in adipose tissue extracted from LysM PTP1B animals compared with controls ($P \leq 0.05$; two-tailed *t* test) and a trend for decreased *CD68* expression ($P = 0.09$; two-tailed *t* test). *K*: Liver triglycerides were significantly lower in LysM PTP1B tissue compared with controls ($P \leq 0.001$; two-tailed *t* test). *L*: Hematoxylin and eosin staining of liver sections show a decreased presence of lipid accumulation in hepatocytes of LysM PTP1B mice (lower panel) compared with control livers (upper panel). *M*: Levels of serum ALT were found to be lower in HF-fed LysM PTP1B mice compared with controls ($P \leq 0.05$; two-tailed *t* test). *N*: Hepatic expression of antiapoptotic mRNA *BCL-2* was significantly upregulated in HF-fed, LPS-treated LysM PTP1B mice compared with controls ($P \leq 0.01$; two-tailed *t* test). Control, white bars or open circles; LysM PTP1B, black bars or closed circles. Data are expressed as mean ± SEM. Prefix "p," phosphorylated; +ve, positive. $^*P < 0.05$, $^{**}P < 0.01$, $^{***}P < 0.001$.

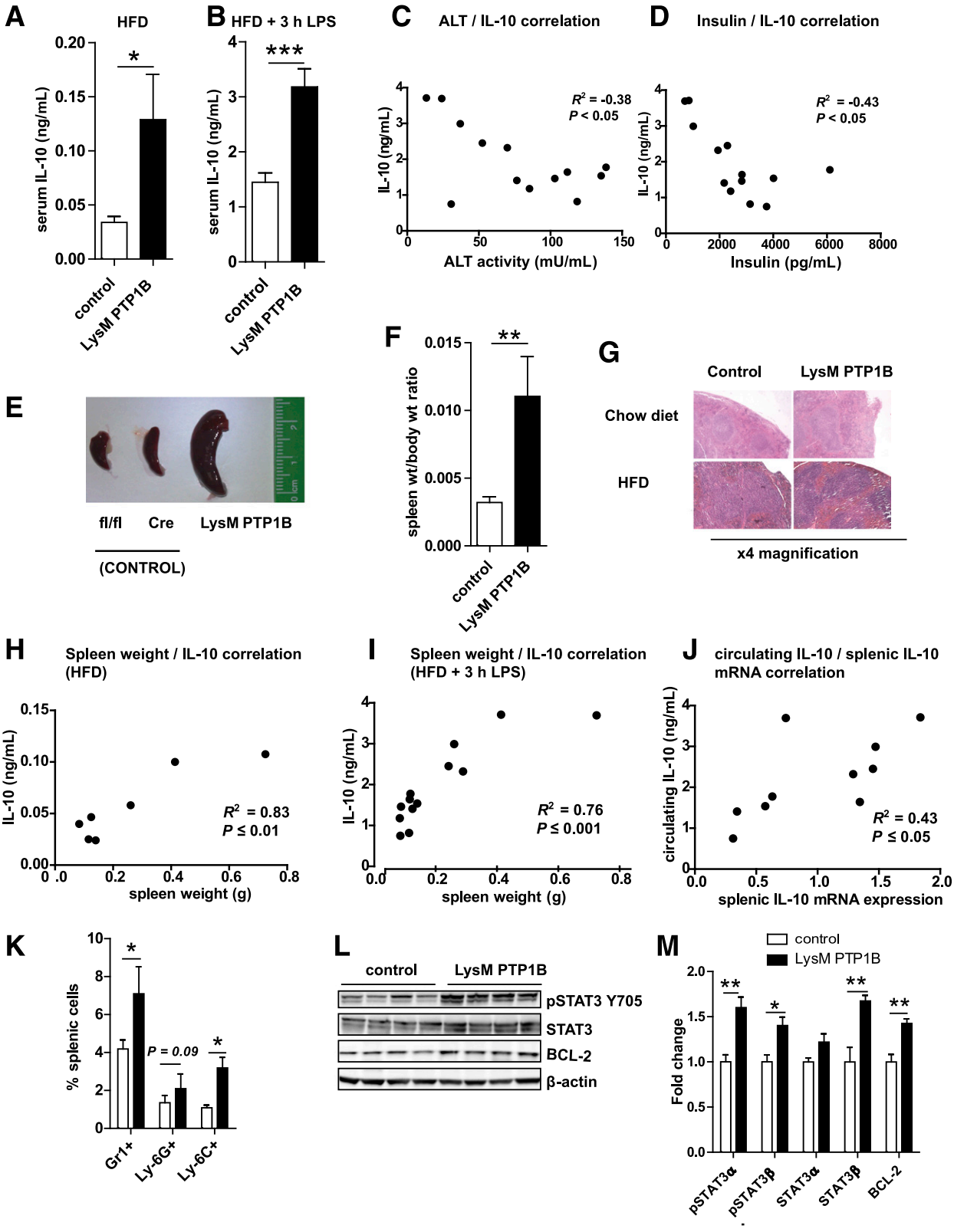

Figure 5—HF-fed LysM PTP1B mice have increased circulating IL-10 likely to originate from enlarged spleens containing elevated myeloid cell numbers and increased phosphorylated STAT3 in vivo. *A* and *B*: Levels of IL-10 were increased in LysM PTP1B mice (n = 4) following long-term HF feeding compared with controls (n = 9; 0.13 ± 0.04 and 0.03 ± 0.006 ng/ml, respectively; $P \leq 0.05$; two-tailed t test) (*A*) and 3 h after receiving an intraperitoneal dose of 0.5 mg/kg LPS (3.18 ± 0.33 and 1.45 ± 0.17 ng/ml, respectively; $P \leq 0.001$; two-tailed t test) (*B*). *C* and *D*: Serum IL-10 levels were found to negatively correlate with ALT activity ($R^2 = -0.38$; $P < 0.05$) (*C*) and circulating insulin ($R^2 = -0.43$; $P < 0.05$) (*D*) levels. *E*: Photographs showing spleens harvested from HF-fed LysM PTP1B mice compared with those from control mice on fl/fl and LysM-Cre backgrounds. *F*: Increased spleen-to-body-weight ratio for HF-fed LysM PTP1B mice

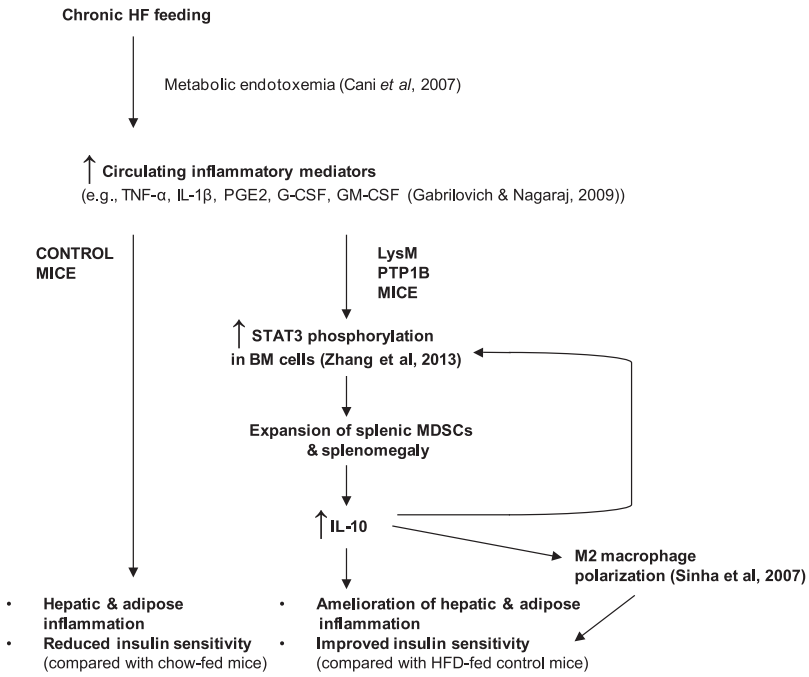

Figure 6—Schematic showing postulated mechanism responsible for the amelioration of hepatic and adipose inflammation leading to improved insulin sensitivity in HF-fed LysM PTP1B mice.

have been associated with obese and insulin-resistant states, as have polymorphisms and haplotypes of the IL-10 promoter, and IL-10 has been shown to mediate insulin-sensitizing effects in adipose, liver, and skeletal muscle by suppressing the deleterious effects of TNF-α and IL-6 on insulin signaling (35–40). Furthermore, a shift toward an alternatively activated, anti-inflammatory M2 macrophage phenotype in adipose tissue has been associated with increased expression of IL-10 (38).

The source of elevated IL-10 in HFD-fed LysM PTP1B mice suggests it to be splenic in origin, due to the close correlations noted between circulating IL-10, spleen size, and splenic *IL-10* mRNA expression. Further analysis of the spleens from these mice revealed an increased expression of the antiapoptotic protein BCL2, which is regulated by *STAT3* and may partly explain the splenomegaly phenotype (41) and an elevation in the alternatively spliced STAT3β isoform. Isoform-specific knockout models have demonstrated that STAT3β plays a crucial role in inhibiting the acute inflammatory responses, whereby mice lacking STAT3β showed increased susceptibility and impaired recovery following in vivo challenge with LPS (42).

Increased phosphorylation of splenic STAT3 found in HFD-fed LysM PTP1B mice is in agreement with our in vitro BMDM studies, as well as a recent study confirming STAT3 as a substrate of myeloid PTP1B (34), which demonstrated that global PTP1B$^{-/-}$ mice are protected against experimental colitis because of a STAT3/JAK2-mediated expansion of myeloid-derived suppressor cells (MDSCs) (34). Our data also provide evidence that this mechanism is, at least in part, applicable to the anti-inflammatory phenotype observed in HFD-fed LysM PTP1B mice. States of chronic inflammation, which could be extended to encompass metabolic endotoxemia, are known to expand immunosuppressive MDSC populations (CD11b+ Gr+ cells) via elevations in factors such as proinflammatory cytokines, prostanoids, and growth factors that lead to persistent STAT3 activation (43). In the absence of myeloid PTP1B, we observe increased phosphorylated STAT3 in the spleen, elevated numbers

compared with controls ($P \leq 0.01$; two-tailed *t* test). *G*: Hematoxylin and eosin staining of spleen sections from representative control and LysM PTP1B mice following HF feeding. *H* and *I*: Spleen weight was found to correlate with circulating *IL-10* levels in pre-LPS ($R^2 = 0.83$; $P \leq 0.01$) (*H*) and post-LPS ($R^2 = 0.76$; $P \leq 0.001$) (*I*) states. *J*: Circulating levels of IL-10 were found to also correlate with levels of splenic *IL-10* mRNA ($R^2 = 0.43$; $P \leq 0.05$). *K*: Flow cytometry analysis of spleen cells revealed an increase in the percentage of cells expressing the monocyte/granulocyte marker Gr1 ($P \leq 0.05$; two-tailed *t* test), the monocyte marker Ly-6C ($P \leq 0.05$; two-tailed *t* test), and the granulocyte marker Ly6G ($P = 0.09$). *L*: Immunoblot displaying increased levels of phosphorylated STAT3α relative to STAT3α ($P \leq 0.01$; two-tailed *t* test), phosphorylated STAT3β relative to STAT3β ($P \leq 0.05$; two-tailed *t* test), STAT3β, and BCL-2 relative to β-actin ($P \leq 0.01$; two-tailed *t* test) and BCL-2 ($P \leq 0.01$; two-tailed *t* test) in spleens harvested from HF-fed LysM PTP1B ($n = 4$) compared with control mice ($n = 4$) as quantified by relative densitometry. *M*: Control, white bars; LysM PTP1B, black bars. Data are expressed as mean ± SEM. Wt, weight; pSTAT, phosphorylated STAT. *$P < 0.05$, **$P < 0.01$, ***$P < 0.001$.

of splenic cells expressing myeloid markers, and marked splenomegaly, which would be indicative of MDSC expansion (43). In addition to the ability of MDSCs to inhibit T-cell activation (44,45) and NK-cell tumor cytotoxicity (46), these cells are known to interact with macrophages by secreting elevated levels of IL-10, which promote macrophage polarization toward the M2 macrophage phenotype (47). It is therefore plausible to postulate that in the absence of myeloid PTP1B, chronic HFD feeding leads to a STAT3-dependent expansion of IL-10–secreting splenic MDSCs and possibly M2 macrophages, which alleviate hepatic and adipose inflammation and enhance insulin sensitivity. Figure 6 displays a schematic depicting the postulated mechanism responsible for the beneficial effects observed for HFD-fed LysM PTP1B mice.

In summary, this study provides evidence that LysM PTP1B mice exhibit improved glucose tolerance and suppressed inflammatory responses in HFD-fed and endotoxemic mouse models. This is contrary to previous reports that have assigned an anti-inflammatory function to macrophage PTP1B and will therefore help allay concerns relating to the application of PTP1B inhibitors in the clinical setting and open up new avenues for the use of PTP1B inhibitors as anti-inflammatory agents.

Acknowledgments. The authors thank Benjamin Neel (University of Toronto), Barbara Kahn (Harvard Medical School), and Kendra Bence (University of Pennsylvania) for providing PTP1B floxed mice and for their continuous mentoring support. The authors also thank Simon Arthur and Vicky McGuire (University of Dundee) for helpful discussions.

Funding. This work was supported by a British Heart Foundation project grant to M.D. (PG/11/8/28703) and a European Foundation for the Study of Diabetes/Lilly Diabetes Programme grant to N.M. and M.D.

Duality of Interest. No potential conflicts of interest relevant to this article were reported.

Author Contributions. L.G. conceived, designed, and performed the experiments and wrote the manuscript. K.D.S. designed and performed the experiments. A.C., E.K.L., C.O., A.A., J.W., and C.M.-G. performed the experiments. J.V.F. and H.M.W. suggested experiments and reviewed the manuscript. N.M. and M.D. conceived and designed the experiments and wrote the manuscript. M.D. is the guarantor of this work and, as such, had full access to all the data in the study and takes responsibility for the integrity of the data and the accuracy of the data analysis.

Prior Presentation. Parts of this study were presented in abstract form at the Diabetes U.K. Professional Conference, Manchester, U.K., 13–15 March 2013.

References

1. Elchebly M, Payette P, Michaliszyn E, et al. Increased insulin sensitivity and obesity resistance in mice lacking the protein tyrosine phosphatase-1B gene. Science 1999;283:1544–1548
2. Klaman LD, Boss O, Peroni OD, et al. Increased energy expenditure, decreased adiposity, and tissue-specific insulin sensitivity in protein-tyrosine phosphatase 1B-deficient mice. Mol Cell Biol 2000;20:5479–5489
3. Bence KK, Delibegovic M, Xue B, et al. Neuronal PTP1B regulates body weight, adiposity and leptin action. Nat Med 2006;12:917–924
4. Delibegovic M, Bence KK, Mody N, et al. Improved glucose homeostasis in mice with muscle-specific deletion of protein-tyrosine phosphatase 1B. Mol Cell Biol 2007;27:7727–7734
5. Delibegovic M, Zimmer D, Kauffman C, et al. Liver-specific deletion of protein-tyrosine phosphatase 1B (PTP1B) improves metabolic syndrome and attenuates diet-induced endoplasmic reticulum stress. Diabetes 2009;58:590–599
6. Owen C, Czopek A, Agouni A, et al. Adipocyte-specific protein tyrosine phosphatase 1B deletion increases lipogenesis, adipocyte cell size and is a minor regulator of glucose homeostasis. PLoS ONE 2012;7:e32700
7. Weisberg SP, McCann D, Desai M, Rosenbaum M, Leibel RL, Ferrante AW Jr. Obesity is associated with macrophage accumulation in adipose tissue. J Clin Invest 2003;112:1796–1808
8. Xu H, Barnes GT, Yang Q, et al. Chronic inflammation in fat plays a crucial role in the development of obesity-related insulin resistance. J Clin Invest 2003;112:1821–1830
9. Hotamisligil GS, Shargill NS, Spiegelman BM. Adipose expression of tumor necrosis factor-alpha: direct role in obesity-linked insulin resistance. Science 1993;259:87–91
10. Jager J, Grémeaux T, Cormont M, Le Marchand-Brustel Y, Tanti JF. Interleukin-1beta-induced insulin resistance in adipocytes through down-regulation of insulin receptor substrate-1 expression. Endocrinology 2007;148:241–251
11. Senn JJ, Klover PJ, Nowak IA, Mooney RA. Interleukin-6 induces cellular insulin resistance in hepatocytes. Diabetes 2002;51:3391–3399
12. Chen A, Mumick S, Zhang C, et al. Diet induction of monocyte chemoattractant protein-1 and its impact on obesity. Obes Res 2005;13:1311–1320
13. Shi H, Kokoeva MV, Inouye K, Tzameli I, Yin H, Flier JS. TLR4 links innate immunity and fatty acid-induced insulin resistance. J Clin Invest 2006;116:3015–3025
14. Saberi M, Woods NB, de Luca C, et al. Hematopoietic cell-specific deletion of toll-like receptor 4 ameliorates hepatic and adipose tissue insulin resistance in high-fat-fed mice. Cell Metab 2009;10:419–429
15. Xu H, An H, Hou J, et al. Phosphatase PTP1B negatively regulates MyD88- and TRIF-dependent proinflammatory cytokine and type I interferon production in TLR-triggered macrophages. Mol Immunol 2008;45:3545–3552
16. Nasimian A, Taheripak G, Gorgani-Firuzjaee S, Sadeghi A, Meshkani R. Protein tyrosine phosphatase 1B (PTP1B) modulates palmitate-induced cytokine production in macrophage cells. Inflamm Res 2013;62:239–246
17. Heinonen KM, Dubé N, Bourdeau A, Lapp WS, Tremblay ML. Protein tyrosine phosphatase 1B negatively regulates macrophage development through CSF-1 signaling. Proc Natl Acad Sci USA 2006;103:2776–2781
18. Clausen BE, Burkhardt C, Reith W, Renkawitz R, Förster I. Conditional gene targeting in macrophages and granulocytes using LysMcre mice. Transgenic Res 1999;8:265–277
19. Ren Y, Xie Y, Jiang G, et al. Apoptotic cells protect mice against lipopolysaccharide-induced shock. J Immunol 2008;180:4978–4985
20. Agouni A, Mody N, Owen C, et al. Liver-specific deletion of protein tyrosine phosphatase (PTP) 1B improves obesity- and pharmacologically induced endoplasmic reticulum stress. Biochem J 2011;438:369–378
21. Agouni A, Owen C, Czopek A, Mody N, Delibegovic M. In vivo differential effects of fasting, re-feeding, insulin and insulin stimulation time course on insulin signaling pathway components in peripheral tissues. Biochem Biophys Res Commun 2010;401:104–111

22. Erwig LP, Kluth DC, Walsh GM, Rees AJ. Initial cytokine exposure determines function of macrophages and renders them unresponsive to other cytokines. J Immunol 1998;161:1983–1988
23. Cani PD, Amar J, Iglesias MA, et al. Metabolic endotoxemia initiates obesity and insulin resistance. Diabetes 2007;56:1761–1772
24. Niemand C, Nimmesgern A, Haan S, et al. Activation of STAT3 by IL-6 and IL-10 in primary human macrophages is differentially modulated by suppressor of cytokine signaling 3. J Immunol 2003;170:3263–3272
25. Heinonen KM, Bourdeau A, Doody KM, Tremblay ML. Protein tyrosine phosphatases PTP-1B and TC-PTP play nonredundant roles in macrophage development and IFN-gamma signaling. Proc Natl Acad Sci USA 2009;106:9368–9372
26. Murray PJ. STAT3-mediated anti-inflammatory signalling. Biochem Soc Trans 2006;34:1028–1031
27. Moore KW, de Waal Malefyt R, Coffman RL, O'Garra A. Interleukin-10 and the interleukin-10 receptor. Annu Rev Immunol 2001;19:683–765
28. Schindler C, Levy DE, Decker T. JAK-STAT signaling: from interferons to cytokines. J Biol Chem 2007;282:20059–20063
29. Myers MP, Andersen JN, Cheng A, et al. TYK2 and JAK2 are substrates of protein-tyrosine phosphatase 1B. J Biol Chem 2001;276:47771–47774
30. Benkhart EM, Siedlar M, Wedel A, Werner T, Ziegler-Heitbrock HW. Role of Stat3 in lipopolysaccharide-induced IL-10 gene expression. J Immunol 2000;165:1612–1617
31. Bourdeau A, Dubé N, Tremblay ML. Cytoplasmic protein tyrosine phosphatases, regulation and function: the roles of PTP1B and TC-PTP. Curr Opin Cell Biol 2005;17:203–209
32. Lu X, Malumbres R, Shields B, et al. PTP1B is a negative regulator of interleukin 4-induced STAT6 signaling. Blood 2008;112:4098–4108
33. Feldhammer M, Uetani N, Miranda-Saavedra D, Tremblay ML. PTP1B: a simple enzyme for a complex world. Crit Rev Biochem Mol Biol 2013;48:430–445
34. Zhang J, Wang B, Zhang W, et al. Protein tyrosine phosphatase 1B deficiency ameliorates murine experimental colitis via the expansion of myeloid-derived suppressor cells. PLoS ONE 2013;8:e70828
35. van Exel E, Gussekloo J, de Craen AJ, Frölich M, Bootsma-Van Der Wiel A, Westendorp RG; Leiden 85 Plus Study. Low production capacity of interleukin-10 associates with the metabolic syndrome and type 2 diabetes: the Leiden 85-Plus Study. Diabetes 2002;51:1088–1092
36. Esposito K, Pontillo A, Giugliano F, et al. Association of low interleukin-10 levels with the metabolic syndrome in obese women. J Clin Endocrinol Metab 2003;88:1055–1058
37. Scarpelli D, Cardellini M, Andreozzi F, et al. Variants of the interleukin-10 promoter gene are associated with obesity and insulin resistance but not type 2 diabetes in caucasian italian subjects. Diabetes 2006;55:1529–1533
38. Lumeng CN, Bodzin JL, Saltiel AR. Obesity induces a phenotypic switch in adipose tissue macrophage polarization. J Clin Invest 2007;117:175–184
39. Hong EG, Ko HJ, Cho YR, et al. Interleukin-10 prevents diet-induced insulin resistance by attenuating macrophage and cytokine response in skeletal muscle. Diabetes 2009;58:2525–2535
40. Kim HJ, Higashimori T, Park SY, et al. Differential effects of interleukin-6 and -10 on skeletal muscle and liver insulin action in vivo. Diabetes 2004;53:1060–1067
41. Ogilvy S, Metcalf D, Print CG, Bath ML, Harris AW, Adams JM. Constitutive Bcl-2 expression throughout the hematopoietic compartment affects multiple lineages and enhances progenitor cell survival. Proc Natl Acad Sci USA 1999;96:14943–14948
42. Yoo JY, Huso DL, Nathans D, Desiderio S. Specific ablation of Stat3beta distorts the pattern of Stat3-responsive gene expression and impairs recovery from endotoxic shock. Cell 2002;108:331–344
43. Gabrilovich DI, Nagaraj S. Myeloid-derived suppressor cells as regulators of the immune system. Nat Rev Immunol 2009;9:162–174
44. Serafini P, De Santo C, Marigo I, et al. Derangement of immune responses by myeloid suppressor cells. Cancer Immunol Immunother 2004;53:64–72
45. Nagaraj S, Gupta K, Pisarev V, et al. Altered recognition of antigen is a mechanism of CD8+ T cell tolerance in cancer. Nat Med 2007;13:828–835
46. Liu C, Yu S, Kappes J, et al. Expansion of spleen myeloid suppressor cells represses NK cell cytotoxicity in tumor-bearing host. Blood 2007;109:4336–4342
47. Sinha P, Clements VK, Bunt SK, Albelda SM, Ostrand-Rosenberg S. Cross-talk between myeloid-derived suppressor cells and macrophages subverts tumor immunity toward a type 2 response. J Immunol 2007;179:977–983

SUPPLEMENTARY DATA

Supplementary Table 1. Gene expression analysis of unstimulated and LPS-stimulated (100ng/ml for 4hr) control and LysM PTP1B BMDMs.

Gene	Treatment	Control	LysM PTP1B	*P* value
		Mean ± sem	Mean ± sem	
IL-12	Unstimulated	1 ± 0.39	1.13 ± 0.07	*0.75*
	4hr LPS	750931 ± 344883	484493 ± 215365	*0.54*
IL-6	Unstimulated	1 ± 0.47	0.02 ± 0.002	*0.08*
	4hr LPS	25927 ± 8029	29967 ± 10838	*0.77*
IL-1β	Unstimulated	1 ± 0.27	30.17 ± 29.31	*0.35*
	4hr LPS	3565223 ± 11968998	4182115 ± 1849572	*0.83*
MCP1	Unstimulated	1 ± 0.91	0.76 ± 0.44	*0.82*
	4hr LPS	49.42 ± 24.68	86.39 ± 41.77	*0.48*
Arginase	Unstimulated	1 ± 0.18	0.91 ± 0.06	*0.66*
	4hr LPS	0.6 ± 0.31	0.79 ± 0.26	*0.65*
CCL17	Unstimulated	1 ± 1	4.61 ± 1.58	*0.1*
	4hr LPS	1507.48 ±702.23	2545.28 ±578.68	*0.3*
CCL22	Unstimulated	1 ± 0.16	0.97 ± 0.15	*0.9*
	4hr LPS	1147.15 ± 489.19	2153.93 ± 792.78	*0.32*
SOCS3	Unstimulated	1 ± 0.18	0.91 ± 0.06	*0.66*
	4hr LPS	79.36 ± 26.67	190.24 ± 94.37	*0.3*
IL-4RA	Unstimulated	1 ± 0.16	1.24 ± 0.24	*0.44*
	4hr LPS	1.04 ± 0.27	1.74 ± 0.60	*0.33*
BCL3	Unstimulated	1 ± 0.54	1 ± 0.39	*1*
	4hr LPS	7.62 ± 1.46	9.69 ± 2.84	*0.54*
BCL2	Unstimulated	1 ± 0.73	0.71 ± 0.29	*0.72*
	4hr LPS	14.22 ± 4.58	43.55 ± 25.67	*0.3*
IKAROS	Unstimulated	1 ± 0.76	0.67 ± 0.29	*0.70*
	4hr LPS	16.42 ± 5.57	55.48 ± 34.50	*0.31*

LysM PTP1B mice (n = 4) versus control mice (n = 4). mRNA expression levels calculated relative to reference genes (β-actin, YWhaz and NoNo). Data expressed as mean ± S.E.M. Significance value taken as $P \leq 0.05$ from two-tailed Student's T-test.

SUPPLEMENTARY DATA

Supplementary Table 2. Flow cytometry data showing percentage spleen cells expressing specific cell markers and corrected for absolute cell numbers.

Marker	% cells expressing marker			Absolute cell no. expressing marker ($x10^7$)		
	Control	LysM PTP1B	Significance level	Control	LysM PTP1B	Significance level
$CD3^+$	28.3 ± 2.2	24.6 ± 1.2	P = 0.3	2.2 ± 0.3	4.2 ± 0.4	**
$B220^+$	54.3 ± 4.2	54.5 ± 3.9	P = 1	4.5 ± 0.3	9.3 ± 0.7	****
$CD11b^+$	6.4 ± 1.0	7.8 ± 2.3	P = 0.5	0.5 ± 0.1	1.4 ± 0.4	*
$CD11c^+$	5.18 ± 0.75	5.60 ± 0.43	P = 0.7	0.5 ± 0.1	1.0 ± 0.2	**
F4/80+	12.5 ± 1.2	16.9 ± 1.6	P = 0.06	1.1 ± 0.2	2.9 ± 0.4	***
$MHCII^+$	65.0 ± 4.6	66.4 ± 4.3	P = 0.9	5.5 ± 0.54	11.3 ± 0.70	****
$Gr1^+$	See *fig 5M*			0.4 ± 0.1	1.3 ± 0.7	**

Flow cytometry was carried out on spleen cells isolated from HFD-fed LysM PTP1B mice (n = 4) and control mice (n = 8). Values on the left side depict the percentage of cells expressing each marker and right side shows total number of cells expressing each marker. Data expressed as mean ± S.E.M. Significance value taken as $P \leq 0.05$ (*), $P \leq 0.01$ (**), $P \leq 0.001$ (***), $P \leq 0.0001$ (****) from two-tailed Student's T-test.

SUPPLEMENTARY DATA

Primer sequences

Arginase F	CAGAAGAATGGAAGAGTCAG
Arginase R	CAGATATGCAGGGAGTCACC
BCL2 F	GGATGACTTCTCTCGTCGTCGCTAC
BCL2 R	TGACATCTCCCTGTTGACGCT
BCL3 F	CCGGAGGCCCTTTACTACCA
BCL3R	GGAGTAGGGGTGAGTAGGCAG
β-actin F	GGGGTGTTGAAGGTCTCAAA
β-actin R	GATCTGGCACCACACACACCTTTCT
CCL17 F	AGTGCTGCCTGGATTACTTCAAAG
CCL17 R	CTGGACAGTCAGAAACACGATGG
CCL22 F	TAACATCATGGCTACCCTGCG
CCL22 R	TGTCTTCCACATTGGCACCA
CD68 F	TGTCTGATCTTGCTAGGACCG
CD68 R	GAGAGTAACGGCCTTTTTGTGA
F4/80 F	CCCAGCTTATGCCACCTGCA
F4/80 R	TCCAGGCCCCTGGAACATTGG
FAS F	GGAGGTGGTGATAGCCGGTAT
FAS R	TGGGTAATCCATAGAGCCCAG
G6Pase F	ATGAACATTCTCCATGACTTTGGG
G6Pase R	GACAGGGAACTGCTTTATTATAGG
IKAROS F	AGACAAGTGCCTGTCAGACAT
IKAROS R	CCAGGTAGTTGATGGCATTGTTG
IL1 beta F	GCAACTGTTCCTGAACTCAACT
IL1 beta R	ATCTTTTGGGGTCCGTCAACT
IL4RA F	TCTGCATCCCGTTGTTTTGC
IL4RA R	GCACCTGTGCATCCTGAATG
IL6 F	TAGTCCTTCCTACCCCAATTTCC
IL6 R	TTGGTCCTTAGCCACTCCTTC
IL10 F	GCTCTTACTGACTGGCATGAG
IL10 R	CGCAGCTCTAGGAGCATGTG
IL12 F	GGAAGCACGGCAGCAGAATA
IL12 R	AACTTGAGGGAGAAGTAGGAATGG

SUPPLEMENTARY DATA

iNOS F	GGAGTGACGGCAAACATGACT
iNOS R	TAGCCAGCGTACCGGATGA
MCP-1 F	TTAAAAACCTGGATCGGAACCAA
MCP-1 R	GCATTAGCTTCAGATTTACGGGT
TNF-alpha F	CCCTCACACTCAGATCATCTTCT
TNF-alpha R	GCTACGACGTGGGCTACAG
NoNo F	GCCAGAATGAAGGCTTGACTAT
NoNo R	TATCAGGGGGAAGATTGCCCA
PEPCK F	GAGATAGCGGCACAAT
PEPCK R	TTCAGAGACTATGCGGTG
SOCS3 F	ACCAGCGCCACTTCTTCACA
SOCS3 R	GTGGAGCATCATACTGGTCC
STAT3 F	CAATACCATTGACCTGCCGAT
STAT3 R	GAGCGACTCAAACTGCCCT
YWhaz F	GAAAAGTTCTTGATCCCCAATGC
YWhaz R	TGTGACTGGTCCACAATTCCTT

Supplementary Figure 1. Immunoblot depicting level of IκBα and phosphorylated c-Jun following LPS stimulation (100 ng/ml LPS for 30, 60, 120 min and 24 hr) of LysM-PTP1B (n = 3 or 4) and control (n = 3 or 4) isolated BMDMs.

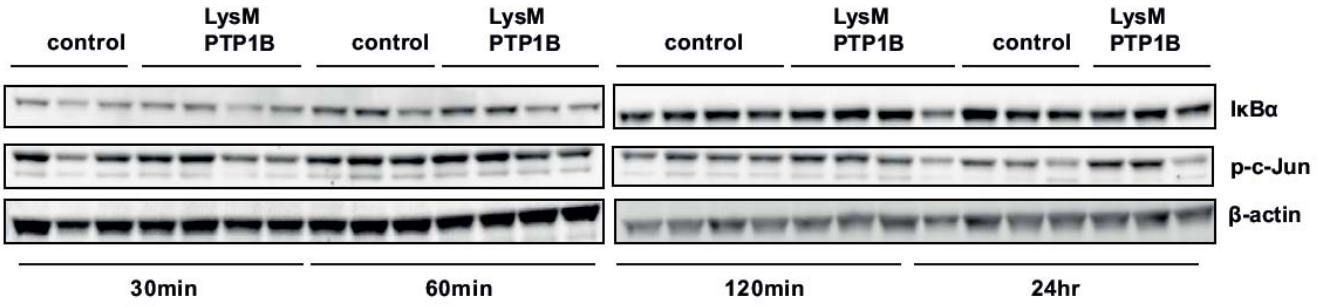

SUPPLEMENTARY DATA

Supplementary Figure 2. Immunoblot depicting levels of phosphorylated ERK 1/2 following LPS stimulation (100 ng/ml LPS for 30 min) of LysM-PTP1B (n = 4) and control (n = 4) isolated BMDMs.

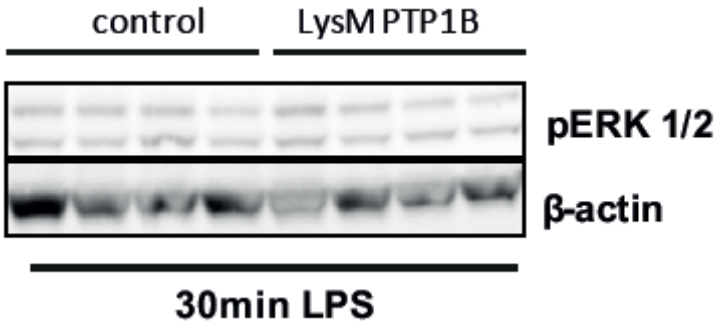

Supplementary Figure 3. Immunoblot depicting levels of phosphorylated IKKα/β, JNK 1/2, and p38 following LPS stimulation (100 ng/ml LPS for 30 min) of LysM-PTP1B (n = 4) and control (n = 4) isolated BMDMs.

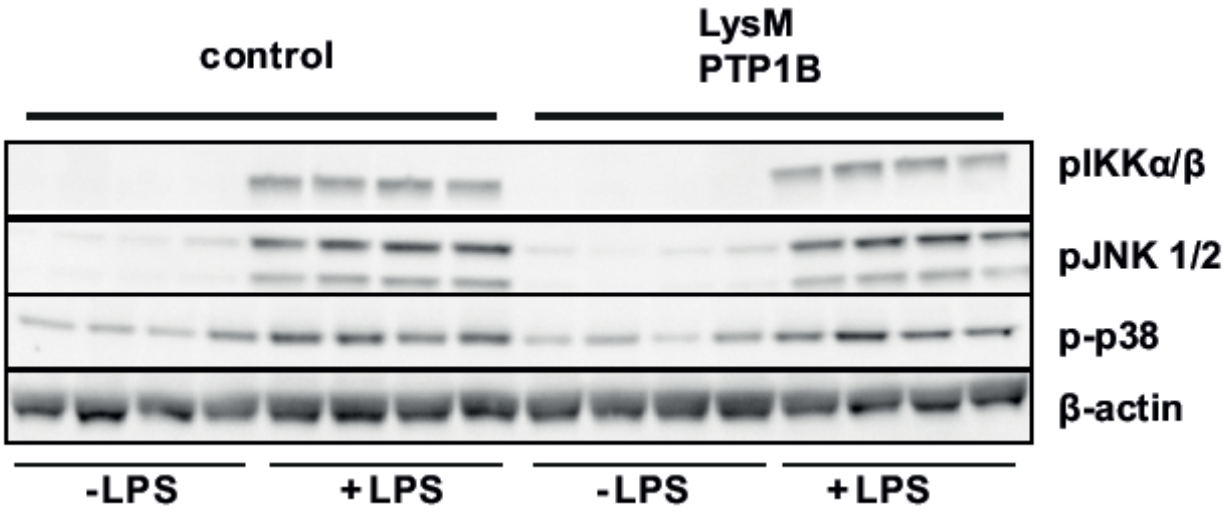

SUPPLEMENTARY DATA

Supplementary Figure 4. Liver insulin signaling immunoblot for saline (control, n = 2; LysM-PTP1B, n = 3) and insulin (control, n = 4; LysM-PTP1B, n = 5) injected mice.

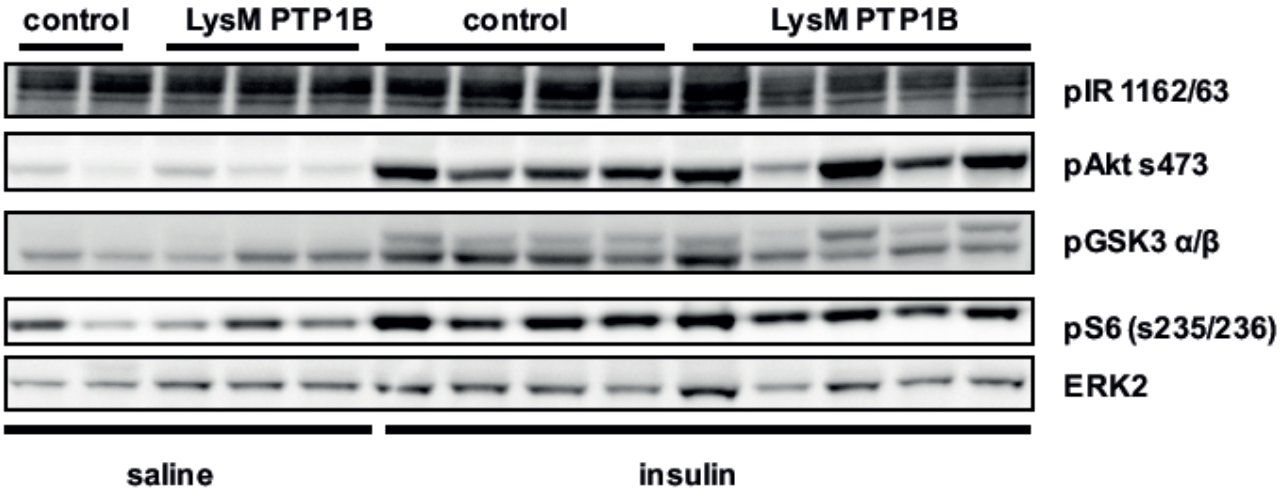

Supplementary Figure 5. WAT insulin signaling immunoblot for saline (control, n = 2; LysM-PTP1B, n = 3) and insulin (control, n = 4; LysM-PTP1B, n = 5) injected mice.

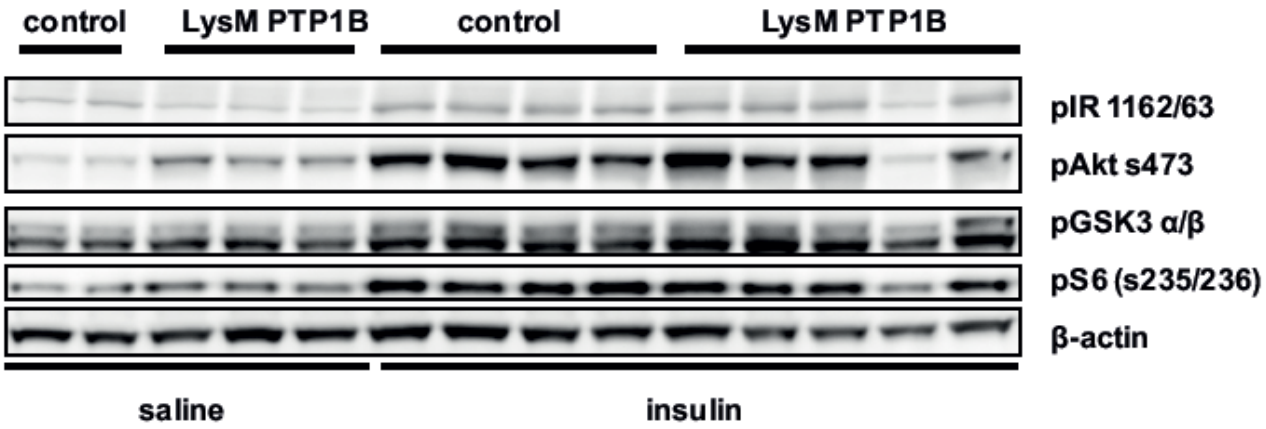

SUPPLEMENTARY DATA

Supplementary Figure 6. Immunohisotchemical staining of adipose tissue from HF-fed control (n=4) and LysM-PTP1B (n=4) with iNOS antibody.